JACS
JOURNAL OF THE AMERICAN CHEMICAL SOCIETY
Article
Cite This: J. Am. Chem. Soc. 2019, 141, 20062−20068
pubs.acs.org/JACS

Enhanced Diffusion and Oligomeric Enzyme Dissociation

Ah-Young Jee,[†] Kuo Chen,[‡,§] Tsvi Tlusty,[†,∥] Jiang Zhao,[‡,§] and Steve Granick*[,†,∥,⊥]

[†]Center for Soft and Living Matter, Institute for Basic Science (IBS), Ulsan 44919, South Korea
[‡]Beijing National Research Center for Molecular Sciences, Institute of Chemistry, Chinese Academy of Sciences, Beijing 100190, China
[§]University of Chinese Academy of Sciences, Beijing 100049, China
[∥]Department of Physics, UNIST, Ulsan 44919, South Korea
[⊥]Department of Chemistry, UNIST, Ulsan 44919, South Korea

Supporting Information

ABSTRACT: The concept that catalytic enzymes can act as molecular machines transducing chemical activity into motion has conceptual and experimental support, but experimental support has involved oligomeric enzymes, often studied under conditions where the substrate concentration is higher than biologically relevant and accordingly exceeds k_M, the Michaelis constant. Urease, a hexamer of subunits, has been considered to be the gold standard demonstrating enhanced diffusion. Here we show that urease and certain other oligomeric enzymes dissociate above k_M into their subunits that diffuse more rapidly, thus providing a simple physical mechanism that contributes to enhanced diffusion in this regime of concentrations. Mindful that this conclusion may be controversial, our findings are supported by four independent analytical techniques: static light scattering, dynamic light scattering (DLS), size-exclusion chromatography (SEC), and fluorescence correlation spectroscopy (FCS). Data for urease are emphasized and the conclusion is validated for hexokinase, acetylcholinesterase, and aldolase. For hexokinase and aldolase no enhanced diffusion is observed except under conditions when these oligomeric enzymes dissociate. At substrate concentration regimes below k_M at which acetylcholinesterase and urease do not dissociate, our finding showing up to 10% enhancement of the diffusion coefficient is consistent with various theoretical scenarios in the literature.

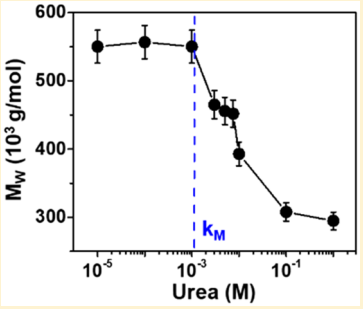

INTRODUCTION

The ubiquity of enzyme catalysis in biology and technology has become even more interesting with the discovery that enzyme catalysis appears to transduce chemical activity into motion leading to enhanced diffusion, a conclusion that came originally from experiments[1−9] and now is buttressed by theoretical analysis.[7,8,10−16] Much of the experimental support comes from considering oligomeric enzymes that evolved to operate within biological cells at substrate concentrations below the Michaelis constant k_M which for urease is ∼3 mM.[17] As many (not all) of the experiments that demonstrate enhanced diffusion operate at significantly larger substrate concentrations than this, it is interesting and relevant to inquire into origins of enhanced diffusion when the substrate concentrations exceed those that are biologically relevant. We focus on urease, which has been considered to be the gold standard demonstrating enhanced diffusion.[1−4,7−9,14,18] The product of urease catalysis is gas whose presence might influence mobility, CO_2. Therefore, to test generality, we also study hexokinase, acetylcholinesterase, and aldolase.

Fluorescence-based measurements of diffusion in the urease system show that it grows in two steps. This enzyme's effective diffusion coefficient measured by fluorescence correlation spectroscopy (FCS) grows smoothly with increasing substrate concentration up to k_M and saturates at a plateau of ∼25% enhancement.[8] To explain this, it was proposed theoretically that the enzyme size shrinks upon substrate binding;[11] alternatively, this laboratory proposed that catalytic chemical activity led to the enhanced mobility.[8] With further increase of substrate concentration a second rise of enhanced diffusion was observed, up to 80%[8] faster than in the absence of substrate. The observation of two-step rise is intriguing because of the higher-concentration regime; having concentrations in the range 0.1−1 M[1−4,14,18] was the condition of many (not all) prior experimental studies. We speculated that the second regime of extra-enhanced diffusion might reflect enzyme dissociation[8] but made no direct test of this hypothesis for this system, though enzyme dissociation into subunits was reported already long ago for F_1-ATPase[19] and more recently, hypothesized for other oligomeric enzymes.[20,21]

Meanwhile, concerns were raised that fluorescence-based measurements might introduce experimental artifact incorrectly interpreted as enhanced diffusion.[9,20−23] This we tested and analyzed elsewhere with a negative conclusion[24] but the dissociation hypothesis was not addressed at that time. With these considerations in mind, here we test directly the enzyme dissociation hypothesis. Mindful that our conclusions may be

Received: July 6, 2019
Published: November 28, 2019

DOI: 10.1021/jacs.9b06949
J. Am. Chem. Soc. 2019, 141, 20062−20068

controversial, we employ four independent analytical techniques: static light scattering, dynamic light scattering (DLS), size-exclusion chromatography (SEC), and fluorescence correlation spectroscopy (FCS). Buffer conditions and other experimental protocols are specified in the Supporting Information.

RESULTS AND DISCUSSION

Choice of Enzyme Samples. To the best of our knowledge, all studies of enhanced diffusion in the urease system concern urease extracted from *Canavalia ensiformis*, the common Jack bean. The source of the urease sample was specified in some studies[1,2,8,25−29] and not specified in other studies,[3,4,7,9,14,18,30,31] as summarized in the Table S1 (Supporting Information). To anticipate conclusions of the following discussion, we found it reassuring that, despite quantitative differences according to which source of urease we used, the qualitative conclusions were the same.

Bearing in mind the doubts recently expressed whether FCS is a true measure of translational diffusion,[9,20−23] we were motivated to perform experiments independent of and complementary to FCS. In order to make the findings most comparable to FCS (fluorescence) measurements on which relied so much earlier data in the literature,[1−4] our principal independent tests were performed on enzymes also labeled in the same manner as for FCS experiments with fluorescent dye using the procedures described in the Supporting Information. Specifically, the light scattering experiments were performed on urease labeled with fluorescent dye.

We now mention some differences between the samples listed in Table S1, especially our finding that the urease of highest catalytic activity aggregated when its concentration exceeded nM. Indeed, the tendency of urease to aggregate in 100 mM PBS buffer (pH 7.2) when the enzyme concentration exceeded 100 nM was noted by us earlier.[7,8] Those experiments were performed using enzymes with the highest purity available to us commercially, Sigma-Aldrich "Type C-3 urease". This presented a difficulty as we wished to respond constructively to the voiced concerns that FCS is artifact,[9,20−23] yet only FCS possesses the sensitivity needed to measure diffusion at nM concentrations. Therefore to assess this sample with our complementary experiments was not feasible.

Of all of the experiments one might use to test the conditions under which oligomeric enzymes might dissociate (Figure 1a), scattering experiments are the most direct as they can give absolute measurements of molar mass. Using the sample of highest catalytic activity, we attempted static light scattering at nM conditions where FCS showed the absence of aggregation, but they failed owing to insufficient sensitivity. Therefore, we turned to using a sample that we found to be less aggregation-prone, Sigma-Aldrich "Type IX". In what follows, we refer to this as sample Ur_1, and to the sample of higher catalytic activity used in our earlier experiments[7,8] as sample Ur_2.

Although control experiments showed the same qualitative conclusions regardless of labeling (Supporting Information), we found that labeling the enzyme with fluorescent dye modulated the catalytic activity, probably by modulating access to the active site. In what follows, we refer to unlabeled and dye-labeled urease as samples Ur_{1u} and Ur_{1f}, respectively. Labeling and purification processes are described in the Supporting Information.

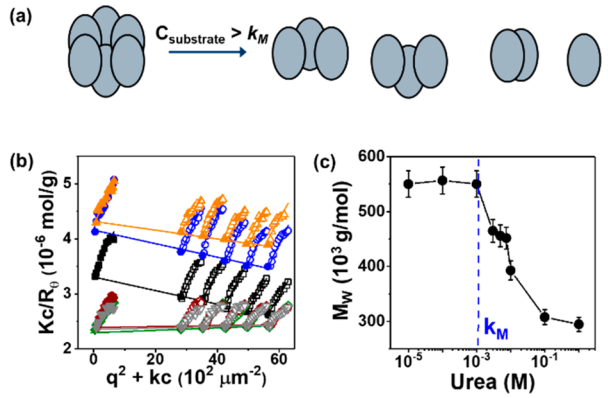

Figure 1. Static light scattering of urease. (a) Schematic diagram in which a multimeric enzyme may dissociate into subunits. (b) Zimm plot for sample Ur_{1f} at various urea concentration where c is mass concentration of enzyme, q is wavevector, and the symbols K, R, and k are constants with standard textbook meanings in static light scattering. K is optical constants, R is the Rayleigh ratio, and k is a constant chosen arbitrarily to shift curves on the x-axis according to the Zimm plot method. Data are open symbols, plotted from top toward bottom at progressively smaller c. Filled symbols denote these data extrapolated to zero concentration. Lines are least-squares fits to the data. Yellow, blue, black, brown, gray, and green shows urea concentration 1, 10^{-1}, 10^{-2}, 10^{-3}, 10^{-4}, and 10^{-5} M in 100 mM PBS buffer (pH 7.2), respectively. (c) Weight-average molecular weight of urease, which is the inverse of the y intercept in panel b, plotted against urea concentration.

Table 1 summarizes the four enzymes studied (urease, acetylcholinesterase, hexokinase, and aldolase). For each enzyme, we show the turnover rate, k_{cat}, and the Michaelis constant, k_M. Sources and experimental procedures are described in the Supporting Information. Figure S1 shows Michaelis−Menten curves for samples Ur_{1f} (urease) and Ac_f (acetylcholinesterase), performed to quantify the enzyme activity.

Table 1. Enzymes Studied and Their Michaelis-Menten Characterization[a]

code	sample	dye	k_{cat} (s^{-1})	k_M (mM)
Ur_{1u}	low activity urease (type IX)	unlabeled	3040	1.04
Ur_{1f}	low activity urease (type IX)	labeled	2,140	1.08
Ur_{2u}	high activity urease (type C-3)	unlabeled	45 020	2.60
Ur_{2f}	high activity urease (type C-3)	labeled	17 020	1.20
Ac_u	acetylcholinesterase (type VI−S)	unlabeled	6100	0.50
Ac_f	acetylcholinesterase (type VI−S)	labeled	4500	0.52
Hex	hexokinase	unlabeled	250[32]	0.20[32]
Ald	aldolase	unlabeled	40[33]	0.05[33]

[a]Characterization was done in this laboratory except when identified by literature reference.[32,33]

Static Light Scattering. First, the absolute weight-average molecular weight (M_w) of urease sample Ur_{1u} was determined using static light scattering.[34] The so-called Zimm plot is the standard way to analyze data of this kind. On the ordinate, a quantity proportional to sample concentration (c) is multiplied by instrumental constants (K) and divided by a measure of scattering at a given specified angle (R_θ). On the abscissa, one plots wavevector squared (q^2) shifted by concentration (kc)

DOI: 10.1021/jacs.9b06949
J. Am. Chem. Soc. 2019, 141, 20062−20068

according to the standard method of fitting, the so-called Zimm plot. Extrapolating both wavevector and concentration to zero, one obtains the y-intercept, which is the inverse weight-average molecular weight, M_w. At substrate concentrations below k_M this gave $M_w = 5.5 \times 10^5$ g mol^{-1} (Da), consistent with the known hexameric form of this enzyme.[17]

The substrate concentration was then increased in small increments by up to 4 orders of magnitude, up to 1 M. It is obvious in Figure 1b that M_w decreases. Inspecting a plot of M_w against substrate concentration (Figure 1c), one sees that M_w is constant below 1 mM but decreases when the substrate concentration is higher. At 1 M concentration the molecular weight is slightly above one-half the original value, suggesting that in the presence of urea, and this enzyme became heavily dissociated. Dissociation into trimers was not complete as M_w slightly exceeded one-half the initial value.

Slopes of Zimm plots quantify pairwise interactions as they are proportional to the second virial coefficient, A_2; positive and negative slopes imply repulsion and attraction, respectively. The negative A_2 at substrate concentrations above 10 mM, more strongly so with increasing substrate concentration, indicates that pairwise attraction grows with increasing concentration (Figure S2), indicating growing tendency toward aggregation. Control FCS measurements described below confirm the same pattern of two-regime enhanced diffusion, below k_M and above it, as reported earlier for sample Ur_{2f}.[8]

Dynamic Light Scattering (DLS). The static light scattering experiments measured molar mass, not mobility. In order to measure diffusion without using FCS, the technique that some studies consider to be problematical,[9,20−23] we turned to dynamic light scattering (DLS). This standard method quantifies the photon autocorrelation function and extracts from it the implied translational diffusion coefficient D. From this, one infers the hydrodynamic radius R_h of an equivalent sphere.[36]

Using sample Ur_{1f}, measurements were made for a relatively short time, as soon as feasible to do after adding substrate (30 s), to minimize the opportunity for aggregation. In the absence of substrate and under conditions of very low substrate concentration, the measured $R_h \approx 8.5$ nm is consistent with literature values for the radius of urease.[35]

Figure 2a compares the autocorrelation $G(t)$ below and above k_M that we determined for this sample (Figure S1). The curve for the latter is shifted to faster time lags indicating faster diffusion, and also shows a two-step process, obvious to the eye in this curve. This contributes to a bimodal distribution when these curves are deconvoluted to show the relative abundance of diffusing entities of different hydrodynamic radius R_h as plotted in Figure 2b. To perform convolution we used the standard CONTIN algorithm.[37] The bimodal distribution at high substrate concentration shows one peak close to the original one, and also a second peak of the size expected if urea dissociates into trimers.

From these distributions we took the peak maxima, calculated their abundance-weighted averages, and plotted these quantities against substrate concentration in Figure 2c. Finally, diffusion coefficients were calculated from the Stokes−Einstein equation. Diffusion enhancement of this enzyme relative to the substrate-free situation is plotted in Figure 2d against substrate concentration. Note the peak from highest R_h, which diminishes with increasing substrate concentration, the peak with lower R_h, which also diminishes with increasing

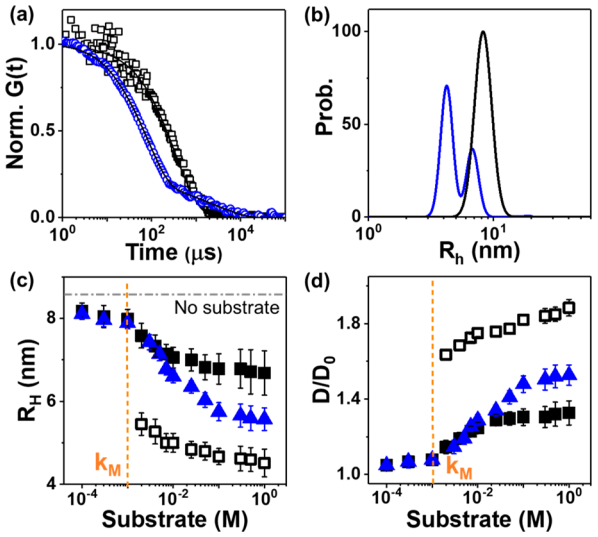

Figure 2. Dynamic light scattering of urease. (a) Photon autocorrelation function of sample Ur_{1f} is plotted against time lag for a representative substrate concentration below k_M (0.1 mM, black) and a representative substrate concentration above k_M (1 M, blue). (b) Distributions of hydrodynamic radius R_h inferred using the CONTIN algorithm from data in panel a. Relative abundance is plotted against radius. The R_h of the black peak is consistent with the reported value.[35] (c) Hydrodynamic radius R_h is plotted against logarithmic substrate concentration across 4 orders of magnitude. Low R_h peak of the bimodal distribution (open symbols), high R_h peak (black) and average R_h weighted by relative abundance (blue) are shown. (d) Relative diffusion coefficients implied from data in panel c are plotted against logarithmic substrate concentration across 4 orders of magnitude. Symbols are same as in panel c.

substrate concentration, and the average inferred from the average R_h.

Size-Exclusion Chromatography (SEC). This standard method to characterize enzyme purity[38] was implemented by us by measuring elution through a Superose 6 SEC column (GE Healthcare), which has a measurement range from 5000 to 5 000 000 Da. The column was calibrated using standard proteins (thyroglobulin, ferritin, and conalbumin), as shown in Figure 3b. This allowed the approximate molecular weight of individual peaks of our unknown sample to be determined.

For sample Ur_{1f}, representative elution curves are plotted in Figure 3a. In the absence of substrate, the SEC chromatogram of urease shows one major peak at elution volume $V_e = 1.6$ mL, and from comparison to the peptide standards this corresponds to 550 000 g mol^{-1}, the molecular weight of urease hexamer. From 5 mM urea and above, a slight shoulder appears on the higher elution side, indicating generation of smaller units. With increasing urea, this becomes a distinct peak centered at 75 000 g mol^{-1}. There are also signs of aggregation. For 100 mM urea, but not yet for 10 mM urea, a second distinct peak appears at $V_e = 1.5$ mL, and this is assigned to 700 000 g mol^{-1}, some kind of aggregate that grew with further increase of urea concentration. Focusing on dissociation of the enzyme into subunits, we deconvoluted the elution peak areas to give relative abundance of hexamers, trimers, and dimers as a function of substrate concentrate, as plotted in Figure 3c.

The time to make measurements using SEC is at least one hour to elute after the sample solution is injected into the column. Unlike the measurements we made using static and

DOI: 10.1021/jacs.9b06949
J. Am. Chem. Soc. 2019, 141, 20062−20068

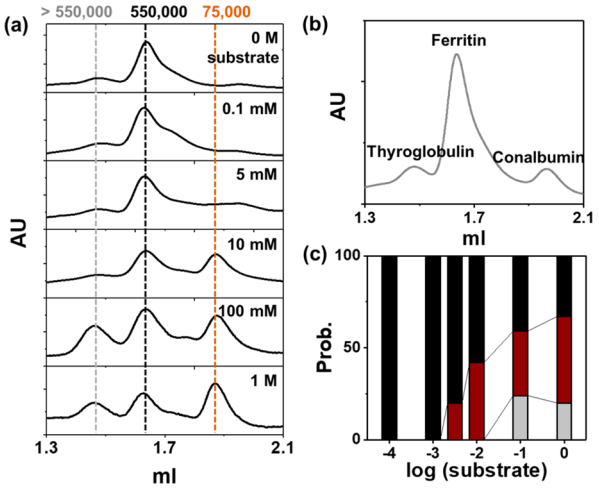

Figure 3. Size-exclusion chromatography of urease in 100 mM PBS buffer (pH 7.2). (a) Chromatograms of sample Ur_{1u} measured on a Superose 6 column. Relative volume eluted through the column is plotted for 6 substrate concentrations, 0 M, 0.1 mM, 5 mM, 10 mM, 100 mM, and 1 M urea, after calibrating the column with standard proteins. (b) Calibration of the SEC column. Elution profiles of Calibration Kit proteins in 100 mM PBS buffer (pH 7.2; standard proteins) on Superpose 6 column. Elution volumes (V_e) are identified with maximum peak height of each respective protein. Thyroglobulin, ferritin, and conalbumin have molar mass 669 000, 440 000, and 75 000 g mol^{-1}, respectively. (c) Relative sizes of the eluted urease, extracted from the peaks of each chromatogram, are plotted against logarithmic substrate concentration. The ordinate of this bar graph shows the relative abundance of the hexamer (black), trimer (red), and dimer (gray). The relatively high enzyme concentration needed for this experiment is believed to explain quantitative differences between Figures 3c and 4d.

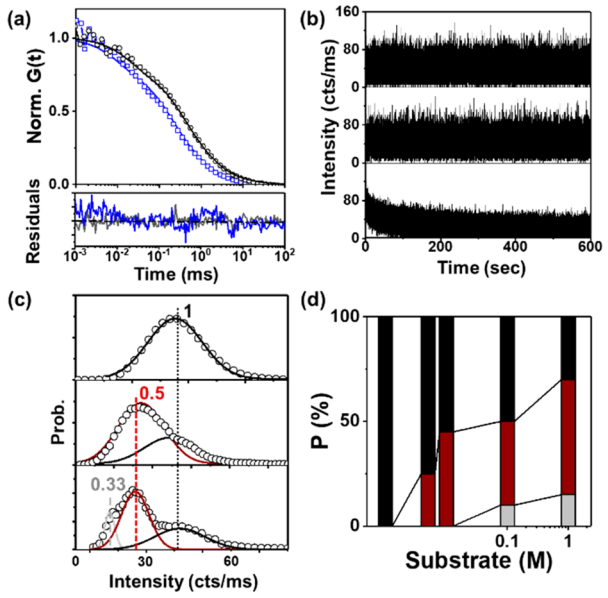

Figure 4. FCS experiments with urease. (a) Normalized autocorrelation function $G(t)$ of Ur_{1f} in 1 mM urea (black) and 100 mM urea (blue) in PBS buffer. The bottom panel shows fitted residuals. (b) Fluorescence intensity time trace of urease with no substrate present; 1 mM urea; and 1 M urea, from top panel to bottom. (c) Fluorescence intensity distribution of urease sample Ur_{1u} at different urea concentration regime. From top panel to bottom panel, it shows 1, 10, and 100 mM of urea, respectively. Black, red, and gray fitting curves represent I_{max}, $1/2I_{max}$, and $1/3I_{max}$ respectively. Binning time, 0.2 ms. (d) The dissociation from hexameric urease to trimer and dimer according to substrate concentration obtained from area fraction of each distribution. Black, red, and gray shows hexamer, trimer, and dimer, respectively.

dynamic light scattering, which were completed within a few minutes, the SEC experiment therefore was more sensitive to the slow process of protein aggregation. The relatively high enzyme concentration needed for this experiment, 200 nM (Supporting Information), is believed to explain quantitative differences between Figures 3c and 4d. Aggregation is suspected to involve denatured urease, but as aggregation was not the point of this study, this matter was not pursued.

Intensity-Weighted FCS. Fluorescence correlation spectroscopy (FCS), a standard method to measure the diffusion of nM-level quantities of molecules including proteins, was used by us and others in earlier studies of enhanced diffusion. However, some studies consider it to be dangerously prone to artifacts from photophysics.[9,20−23] Our systematic test did not support this hypothesis.[24] In this context, it was interesting and relevant to inquire whether FCS measurements are consistent with the other analytical techniques. Our conclusion is that they are consistent.

The measured autocorrelation curves $G(t)$ nicely fit a free diffusion fitting model regardless of urea concentration, except that upon inspecting the fitting residuals for high urea concentration, small systematic deviations are observed at the most rapid time scales, faster than hundreds of microseconds (Figure 4a). As this time scale is a minor contribution to the overall fit, one-component fitting was used.

Raw data from this experiment consists of fluorescence intensity traces as a function of time. In fact, perfect dye labeling efficiency is impossible, but the labeling protocol uses an excess of dye, so for the following argument we assume that the dye has labeled all subunits. To the extent this argument holds, it is therefore relevant to consider how raw values of the fluorescence intensity may change.

The intensity was time-independent during measurements in buffer and 1 mM urea. On the other hand, the intensity gradually diminished over time in the presence of 1 M urea (Figure 4b). Pursuing these differences and using sample Ur_{1f} in the absence of substrate and at substrate concentrations below k_M, we observed a nearly-Gaussian intensity distribution. For higher substrate concentrations this became progressively broader, so we deconvoluted the intensity distributions as illustrated in Figure 4c. The idea behind deconvolution was that if unperturbed urease hexamer enzymes are uniformly labeled to display intensity I_{max} when passing through the FCS confocal spot, dissociated trimers will display $(1/2)I_{max}$ and dimers will display $(1/3)I_{max}$. Deconvolution was performed according to this reasoning. As a function of substrate concentration, the fluorescence intensity was separated into relative abundance of hexamers, trimers, and dimers, as plotted in Figure 4d.

A technical point is that in this analysis, certain quantitative differences can result depending on how the intensity traces are binned according to time. Single Gaussian and bimodal distributions are a robust conclusion regardless of binning size at 1 and 10 mM urea, which are conditions where urease has experienced little dissociation into subunits. On the other hand, when considering the 100 mM substrate concentration, 1 ms binning caused self-averaging of short-time events. Under this condition, we found that binning at 0.2 ms revealed a

DOI: 10.1021/jacs.9b06949
J. Am. Chem. Soc. 2019, 141, 20062−20068

trimodal rather than the bimodal distribution implied by 1 ms binning. These considerations are believed to be why intensity traces do not show evident of the smallest oligomeric subunits, monomers and dimers (Figure S3).

Acetylcholinesterase. Urea is a common protein denaturation agent,[39,40] a fact that potentially might influence the action of urea on the enzyme urease despite the fact that urease has been considered a model system in which to study enhanced diffusion. With this in mind, generality of these findings was checked regarding acetylcholinesterase (AChE), another oligomeric enzyme that in the literature was interpreted to display enhanced diffusion at substrate concentrations above k_M.[7] AChE is a tetramer and its substrate is acetylcholine. We denote the unlabeled and dye-labeled samples as Ac_u and Ac_f, respectively. Studying sample Ac_f, this enzyme's hydrodynamic radius was measured by DLS and the distributions of R_h were inferred when the substrate concentration was increased to values well above k_M. As shown in Figure 5, these data show dissociation of R_h into

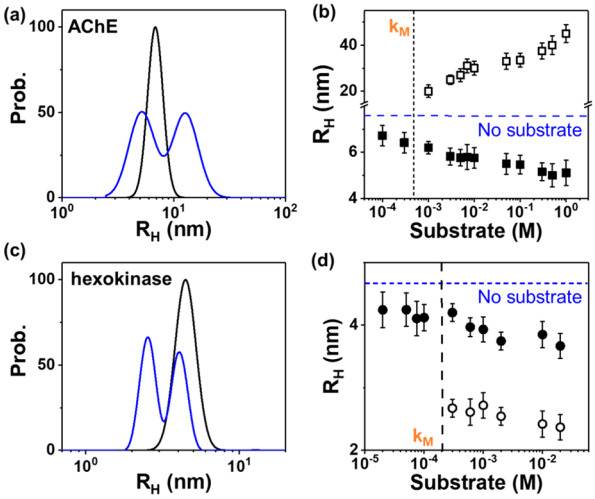

Figure 5. Dynamic light scattering of acetylcholinesterase (AChE) and hexokinase. (a) For AChE sample Ac_u, hydrodynamic radius distribution R_h inferred from autocorrelation curves using the CONTIN algorithm, showing a single peak for 0.3 mM substrate (black) and a bimodal distribution for 1 M substrate (blue). (b) For AChE, hydrodynamic radius R_h is plotted against logarithmic substrate concentration. The measured k_M is shown as a dotted vertical line. (c) For hexokinase sample Ald, hydrodynamic radius distribution R_h inferred from autocorrelation curves using the CONTIN algorithm, showing a single peak for 0.02 mM substrate (black) and a bimodal distribution for 20 mM substrate (blue). (d) For hexokinase, the hydrodynamic radius R_h is plotted against logarithmic substrate concentration. The k_M is shown as a dotted vertical line.

values symptomatic of oligomer dissociation, accompanied by a tendency to aggregate, which is the same dissociation pattern as for urease.

Hexokinase. Hexokinase I, a dimeric enzyme of size 104 000 g/mol used in several earlier studies for which enhanced diffusion was reported at substrate concentrations above k_M was also investigated.[5] The substrate is glucose. This enzyme's hydrodynamic radius was measured by DLS and the distributions of R_h were inferred when the substrate concentration was increased to values well above k_M. The data are similar to those presented above for urease and acetylcholinesterase (Figure 5). Regarding enhanced diffusion, the data obtained by FCS at high substrate concentrations are intermediate between the D/D_0 of the undissociated enzyme and its dissociated components, as expected of this measurement that does not distinguish between them (Figure S4).

Aldolase. The glycolytic enzyme aldolase was also considered in earlier reports of enhanced diffusion.[11] A tetramer, its substrate is fructose-1,6-bisphosphate (FBP), and k_M = 50 μM.[33] This enzyme's hydrodynamic radius was measured by DLS and the distributions of R_h were inferred. As shown in Figure 6, these data depended on reaction time.

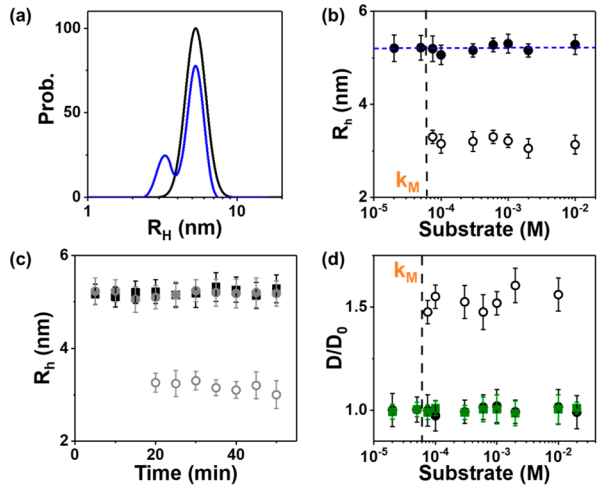

Figure 6. Dynamic light scattering of aldolase. (a) Hydrodynamic radius distribution R_h inferred from autocorrelation curves using the CONTIN algorithm for 50 nM aldolase in the presence of 10 mM substrate (fructose-1,6-bisphosphate, FBP) in 50 mM HEPES buffer, showing a single peak during the initial 20 min reaction time (black) and the period 20−30 min reaction time (blue). (b) Hydrodynamic radius R_h is plotted against logarithmic substrate concentration, showing separately the two peaks of the bimodal distribution after 20 min reaction time. The k_M is shown as a dotted vertical line. (c) Hydrodynamic radius R_h is plotted against reaction for 0.02 mM FBP (black) and 10 mM FBP (gray). (d) Relative diffusion coefficients are plotted against logarithmic substrate concentration for data in panel b (black) and from FCS measurements acquired during the initial 10 min reaction time (green).

During the initial 20 min of reaction the R_h was unperturbed (Figure 6a−c). The diffusion coefficient measured by FCS was similarly unperturbed (Figure 6d). But later the R_h distribution became bimodal (Figure 6a-c). This oligomeric enzyme dissociated as did the other enzymes, but more slowly.

Comparing Enzymes with Different Commercial Provenance. The remaining samples in Table 1 were also studied for completeness. Their Michaelis−Menten characterization is shown in Figure S5.

For urease, DLS experiments are compared for samples Ur_{1u} (Figure S6) and Ur_{2f} (Figure S7). For each, the enzyme's hydrodynamic radius was measured by DLS and the distributions of R_h were inferred when the substrate concentration was increased to values well above k_M. Between these samples there is excellent qualitative consistency but with quantitative differences. These may reflect differences of turnover rate. The biochemical differences that account for different catalytic efficiency were beyond the scope of the present study, but on physical grounds we expect them to involve differences in access of substrate to the active site.

DOI: 10.1021/jacs.9b06949
J. Am. Chem. Soc. 2019, 141, 20062−20068

For acetylcholinesterase, similar comparisons were made for a sample unlabeled with fluorescent dye, sample Ac_u (Figure S8). Between the samples there is also excellent qualitative consistency.

Comparing Dynamic Measurements. Figure 7 compares the diffusion coefficients D inferred for urease from

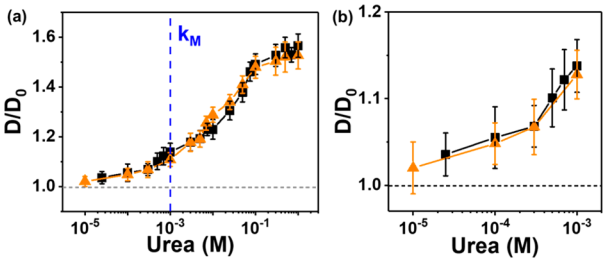

Figure 7. Comparison of DLS and FCS measurements for urease sample Ur_{1f}. Black and orange show findings from FCS and DLS, respectively.

dynamic light scattering and FCS. From these independent techniques, on the same scale all of the D are plotted against logarithmic substrate concentration, over 5 orders of magnitude of substrate concentration in Figure 7a. Substrate concentrations below k_M are magnified in Figure 7b. All measurements appear to agree when the substrate concentration exceeds k_M. For substrate concentrations below k_M, the regime in which the enzyme does not dissociate, FCS and dynamic light scattering agree in showing enhanced diffusion.

CONCLUSIONS

Dissociation of oligomeric enzymes into subunits can contribute to explaining reported instances of enhanced diffusion though they do not exclude contribution from other scenarios that have been advanced theoretically.[8,10−16] It is interesting to speculate about the biological function of this enzyme dissociation phenomenon. Not known presently is whether this question has functional significance, as such high concentrations are not believed to occur in natural settings. It might function as a biological regulatory mechanism.

At the same time, in the regime of biologically relevant substrate concentrations below k_M, we do observe that the presence of substrate enhances diffusion of oligomeric enzymes. This is broadly consistent with the qualitative conclusion from much previous work and helps to clarify the regime of their potential validity.[1−16]

This study is not believed to be directly relevant to an interesting parallel family of studies in which catalytically active enzymes, urease in many instances,[1−4,7−9,14,18,25−31] were attached chemically to the surfaces of colloidal beads or nanoparticles. Enhanced mobility or ballistic motion of colloidal beads is observed when substrate is added.[4,25−31] It is unknown how the methods of enzyme surface-attachment might influence the opportunities for enzyme dissociation into subunits, however. Also enzyme-driven colloids are surely influenced by diffusiophoresis produced by a concentration gradient of reaction products near the surfaces of colloidal beads.[41−44] Diffusiophoresis is not believed to contribute to the situations, considered here, of enzymes at nM concentrations.

ASSOCIATED CONTENT

Supporting Information

The Supporting Information is available free of charge at https://pubs.acs.org/doi/10.1021/jacs.9b06949.

Experimental detail, enzyme assays, and more DLS results of various samples (PDF)

AUTHOR INFORMATION

Corresponding Author

*sgranick@ibs.re.kr

ORCID

Jiang Zhao: 0000-0001-7788-2708

Steve Granick: 0000-0003-4775-2202

Notes

The authors declare no competing financial interest.

ACKNOWLEDGMENTS

This work was supported by the taxpayers of South Korea through the Institute for Basic Science, Project Code IBS-R020-D1. For instrument access we thank IBS-R0190D for dynamic light scattering and IBS-R022-D1 for size exclusion chromatography. We are indebted to Dr. Hyun Suk Kim in the IBS Center for Genomic Integrity for help with SEC measurements.

REFERENCES

(1) Muddana, H. S.; Sengupta, S.; Mallouk, T. E.; Sen, A.; Butler, P. J. Substrate catalysis enhances single-enzyme diffusion. *J. Am. Chem. Soc.* **2010**, *132* (7), 2110−2111.

(2) Sengupta, S.; Dey, K. K.; Muddana, H. S.; Tabouillot, T.; Ibele, M. E.; Butler, P. J.; Sen, A. Enzyme molecules as nanomotors. *J. Am. Chem. Soc.* **2013**, *135* (4), 1406−1414.

(3) Riedel, C.; Gabizon, R.; Wilson, C. A.; Hamadani, K.; Tsekouras, K.; Marqusee, S.; Pressé, S.; Bustamante, C. The heat released during catalytic turnover enhances the diffusion of an enzyme. *Nature* **2015**, *517* (7533), 227.

(4) Dey, K. K.; Zhao, X.; Tansi, B. M.; Méndez-Ortiz, W. J.; Córdova-Figueroa, U. M.; Golestanian, R.; Sen, A. Micromotors powered by enzyme catalysis. *Nano Lett.* **2015**, *15* (12), 8311−8315.

(5) Zhao, X.; Palacci, H.; Yadav, V.; Spiering, M. M.; Gilson, M. K.; Butler, P. J.; Hess, H.; Benkovic, S. J.; Sen, A. Substrate-driven chemotactic assembly in an enzyme cascade. *Nat. Chem.* **2018**, *10* (3), 311.

(6) Zhao, X.; Gentile, K.; Mohajerani, F.; Sen, A. Powering motion with enzymes. *Acc. Chem. Res.* **2018**, *51* (10), 2373−2381.

(7) Jee, A.-Y.; Dutta, S.; Cho, Y.-K.; Tlusty, T.; Granick, S. Enzyme leaps fuel antichemotaxis. *Proc. Natl. Acad. Sci. U. S. A.* **2018**, *115* (1), 14−18.

(8) Jee, A.-Y.; Cho, Y.-K.; Granick, S.; Tlusty, T. Catalytic enzymes are active matter. *Proc. Natl. Acad. Sci. U. S. A.* **2018**, *115* (46), E10812−E10821.

(9) Xu, M.; Ross, J. L.; Valdez, L.; Sen, A. Direct single molecule imaging of enhanced enzyme diffusion. *Phys. Rev. Lett.* **2019**, *123* (12), 128101.

(10) Weistuch, C.; Presse, S. Spatiotemporal organization of catalysts driven by enhanced diffusion. *J. Phys. Chem. B* **2018**, *122* (21), 5286−5290.

(11) Illien, P.; Zhao, X.; Dey, K. K.; Butler, P. J.; Sen, A.; Golestanian, R. Exothermicity is not a necessary condition for enhanced diffusion of enzymes. *Nano Lett.* **2017**, *17* (7), 4415−4420.

(12) Agudo-Canalejo, J.; Adeleke-Larodo, T.; Illien, P.; Golestanian, R. Enhanced diffusion and chemotaxis at the nanoscale. *Acc. Chem. Res.* **2018**, *51* (10), 2365−2372.

DOI: 10.1021/jacs.9b06949
J. Am. Chem. Soc. 2019, 141, 20062−20068

(13) Agudo-Canalejo, J.; Illien, P.; Golestanian, R. Phoresis and enhanced diffusion compete in enzyme chemotaxis. *Nano Lett.* **2018**, *18* (4), 2711−2717.
(14) Mohajerani, F.; Zhao, X.; Somasundar, A.; Velegol, D.; Sen, A. A theory of enzyme chemotaxis: from experiments to modeling. *Biochemistry* **2018**, *57* (43), 6256−6263.
(15) Gaspard, P.; Kapral, R. Thermodynamics and statistical mechanics of chemically powered synthetic nanomotors. *Adv. Phys-X* **2019**, *4* (1), 1602480.
(16) Robertson, B.; Huang, M.-J.; Chen, J.-X.; Kapral, R. Synthetic Nanomotors: Working Together through Chemistry. *Acc. Chem. Res.* **2018**, *51* (10), 2355−2364.
(17) Krajewska, B.; Ureases, I. Functional, catalytic and kinetic properties: A review. *J. Mol. Catal. B: Enzym.* **2009**, *59* (1−3), 9−21.
(18) Zhao, X.; Dey, K. K.; Jeganathan, S.; Butler, P. J.; Córdova-Figueroa, U. M.; Sen, A. Enhanced diffusion of passive tracers in active enzyme solutions. *Nano Lett.* **2017**, *17* (8), 4807−4812.
(19) Shah, N. B.; Hutcheon, M. L.; Haarer, B. K.; Duncan, T. M. F1-ATPase of Escherichia coli: The ϵ-Inhibitied State Forms After ATP Hydrolysis, Is Distinct From The ADP-Inhibited State, And Responds Dynamically To Catalytic Site Ligands. *J. Biol. Chem.* **2013**, *288* (13), 9383−9395.
(20) Zhang, Y.; Armstrong, M. J.; Bassir Kazeruni, N. M.; Hess, H. Aldolase does not show enhanced diffusion in dynamic light scattering experiments. *Nano Lett.* **2018**, *18* (12), 8025−8029.
(21) Günther, J.-P.; Börsch, M.; Fischer, P. Diffusion measurements of swimming enzymes with fluorescence correlation spectroscopy. *Acc. Chem. Res.* **2018**, *51* (9), 1911−1920.
(22) Bai, X.; Wolynes, P. G. On the hydrodynamics of swimming enzymes. *J. Chem. Phys.* **2015**, *143* (16), 165101.
(23) Günther, J.-P.; Majer, G.; Fischer, P. Absolute diffusion measurements of active enzyme solutions by NMR. *J. Chem. Phys.* **2019**, *150* (12), 124201.
(24) Kandula, H. N.; Jee, A.-Y.; Granick, S. Robustness of FCS (Fluorescence Correlation Spectroscopy) with Quenchers Present. *J. Phys. Chem. A* **2019**, *123* (46), 10184−10189.
(25) Ma, X.; Wang, X.; Hahn, K.; Sánchez, S. Motion control of urea-powered biocompatible hollow microcapsules. *ACS Nano* **2016**, *10* (3), 3597−3605.
(26) Ma, X.; Hortelao, A. C.; Miguel-López, A.; Sánchez, S. Bubble-free propulsion of ultrasmall tubular nanojets powered by biocatalytic reactions. *J. Am. Chem. Soc.* **2016**, *138* (42), 13782−13785.
(27) Arqué, X.; Romero-Rivera, A.; Feixas, F.; Patiño, T.; Osuna, S.; Sánchez, S. Intrinsic enzymatic properties modulate the self-propulsion of micromotors. *Nat. Commun.* **2019**, *10* (1), 2826.
(28) Hortelão, A. C.; Patiño, T.; Perez-Jiménez, A.; Blanco, À.; Sánchez, S. Enzyme-Powered Nanobots Enhance Anticancer Drug Delivery. *Adv. Funct. Mater.* **2018**, *28* (25), 1705086.
(29) Patino, T.; Porchetta, A.; Jannasch, A.; Lladó, A.; Stumpp, T.; Schäffer, E.; Ricci, F.; Sánchez, S. Self-Sensing Enzyme-Powered Micromotors Equipped with pH-Responsive DNA Nanoswitches. *Nano Lett.* **2019**, *19* (6), 3440−3447.
(30) Ma, X.; Jannasch, A.; Albrecht, U.-R.; Hahn, K.; Miguel-López, A.; Schäffer, E.; Sánchez, S. Enzyme-powered hollow mesoporous Janus nanomotors. *Nano Lett.* **2015**, *15* (10), 7043−7050.
(31) Patiño, T.; Feiner-Gracia, N.; Arqué, X.; Miguel-López, A.; Jannasch, A.; Stumpp, T.; Schäffer, E.; Albertazzi, L.; Sánchez, S. Influence of enzyme quantity and distribution on the self-propulsion of non-Janus urease-powered micromotors. *J. Am. Chem. Soc.* **2018**, *140* (25), 7896−7903.
(32) Recht, M. I.; Torres, F. E.; De Bruyker, D.; Bell, A. G.; Klumpp, M.; Bruce, R. H. Measurement of enzyme kinetics and inhibitor constants using enthalpy arrays. *Anal. Biochem.* **2009**, *388* (2), 204−212.
(33) Labbé, G.; de Groot, S.; Rasmusson, T.; Milojevic, G.; Dmitrienko, G. I.; Guillemette, J. G. Evaluation of four microbial Class II fructose 1, 6-bisphosphate aldolase enzymes for use as biocatalysts. *Protein Expression Purif.* **2011**, *80* (2), 224−233.
(34) Schärtl, W. *Light scattering from polymer solutions and nanoparticle dispersions*; Springer: Berlin, 2007.
(35) Follmer, C.; Pereira, F. V.; da Silveira, N. P.; Carlini, C. R. Jack bean urease (EC 3.5. 1.5) aggregation monitored by dynamic and static light scattering. *Biophys. Chem.* **2004**, *111* (1), 79−87.
(36) Segrè, P. N.; Meeker, S. P.; Pusey, P. N.; Poon, W. C. K. Viscosity and Structural Relaxation in Suspensions of Hard-Sphere Colloids. *Phys. Rev. Lett.* **1995**, *75* (5), 958−961.
(37) Provencher, S. W. CONTIN: a general purpose constrained regularization program for inverting noisy linear algebraic and integral equations. *Comput. Phys. Commun.* **1982**, *27* (3), 229−242.
(38) Dunn, B. E.; Campbell, G. P.; Perez-Perez, G. I.; Blaser, M. J. Purification and characterization of urease from Helicobacter pylori. *J. Biol. Chem.* **1990**, *265* (16), 9464−9469.
(39) Brandts, J. F.; Hunt, L. Thermodynamics of protein denaturation. III. Denaturation of ribonuclease in water and in aqueous urea and aqueous ethanol mixtures. *J. Am. Chem. Soc.* **1967**, *89* (19), 4826−4838.
(40) Das, A.; Mukhopadhyay, C. Urea-mediated protein denaturation: a consensus view. *J. Phys. Chem. B* **2009**, *113* (38), 12816−12824.
(41) Golestanian, R.; Liverpool, T. B.; Ajdari, A. Propulsion of a molecular machine by asymmetric distribution of reaction products. *Phys. Rev. Lett.* **2005**, *94* (22), 220801.
(42) Howse, J. R.; Jones, R. A.; Ryan, A. J.; Gough, T.; Vafabakhsh, R.; Golestanian, R. Self-motile colloidal particles: from directed propulsion to random walk. *Phys. Rev. Lett.* **2007**, *99* (4), No. 048102.
(43) Ibele, M.; Mallouk, T. E.; Sen, A. Schooling behavior of light-powered autonomous micromotors in water. *Angew. Chem., Int. Ed.* **2009**, *48* (18), 3308−3312.
(44) Tătulea-Codrean, M.; Lauga, E. Artificial chemotaxis of phoretic swimmers: Instantaneous and long-time behaviour. *J. Fluid Mech.* **2018**, *856*, 921−957.

DOI: 10.1021/jacs.9b06949
J. Am. Chem. Soc. 2019, 141, 20062−20068